Vol. 31 (2000) *ACTA PHYSICA POLONICA B* No 10–11

EVIDENCE FOR EXOTIC MESON PRODUCTION IN $\pi^- p$ INTERACTIONS AT 18 GeV/c*

H.J. Willutzki

For the E852 Collaboration †

Brookhaven National Laboratory
Upton, NY 11973, USA

(Received July 13, 2000)

The $\eta\pi^-$ system has been studied in the reaction $\pi^- p \to \eta\pi^- p$ at 18 GeV/c. A large asymmetry in the angular distribution is observed indicating interference between L-even and L-odd partial waves. The data require interference between the $a_2(1320)$ and an exotic $J^{PC} = 1^{-+}$ resonance $\pi_1(1400)$ with $M = (1370 \pm 16^{+50}_{-30})$ MeV/c^2 and $\Gamma = (385 \pm 40^{+65}_{-105})$ MeV/c^2. A second exotic $J^{PC} = 1^{-+}$ resonance $\pi_1(1600)$ has been found in the reaction $\pi^- p \to \pi^+\pi^-\pi^- p$ in the $\rho\pi$ channel. A mass-dependent fit yields $M = (1593 \pm 8^{+29}_{-47})$ MeV/c^2 and $\Gamma = (168 \pm 20^{+150}_{-12})$ MeV/c^2. Presumably the same resonance is also found in the $\eta'(959)\pi^-$ final state with $M = (1589 \pm 9)$ MeV/c^2 and $\Gamma = (380 \pm 22)$ MeV/c^2.

PACS numbers: 12.39.Mk, 13.25.Jx, 13.85.Hd, 14.40.Cs

1. Introduction

According to the quark model a $q\overline{q}$ meson with orbital momentum l and total spin s must have parity $P = (-)^{l+1}$ and charge conjugation $C = (-)^{l+s}$. This excludes states with $J^{PC} = 0^{--}, 0^{+-}, 1^{-+}, 2^{+-}, 3^{-+}$*etc.* Resonances with these exotic quantum numbers could be hybrids, states consisting of a quark, an antiquark and a gluon; or multiquark states.

The properties of exotic states have been predicted by several models [1–7]. These models include the bag model which predicts $J^{PC} = 1^{-+}$ hybrids with masses around 1.4 GeV/c^2, the flux tube model which has

* Presented at the Meson 2000, Sixth International Workshop on Production, Properties and Interaction of Mesons, Cracow, Poland, May 19–23, 2000.

† The E852 collaborating institutions are: Brookhaven, Carnegie Mellon, Indiana, IHEP Protvino, Massachusetts Dartmouth, Moscow State, Northwestern, Notre Dame, Rensselaer Polytechnic Institute, and TJNAF.

masses of hybrids near 1.8 GeV/c^2 and lattice gauge calculations [8] with estimates for hybrid masses between 1.7 GeV/c^2 and 2.1 GeV/c^2.

Experiment E852 was performed at the Multi-Particle Spectrometer facility (MPS) at Brookhaven National Laboratory (BNL). The experiment took data in 1994 (2.47×10^6 triggers), 1995 (8.12×10^6 triggers), 1997 (2.56×10^6 triggers) and 1998 (6.23×10^6 triggers). A detailed description of the apparatus can be found in [9].

2. Study of the reaction $\pi^- p \to \eta\pi^- p$

In this data set of 47 200 events (94 data) the η was detected through its 2γ decay mode, see Fig. 1(a).

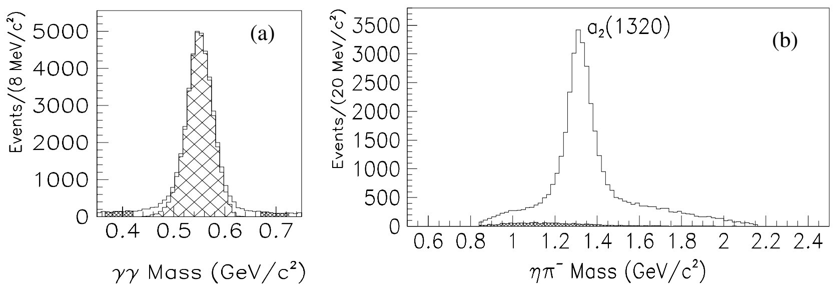

Fig. 1. (a) Two-photon effective mass distribution. The central cross-hatched region shows the events which remain after kinematic fitting. The shaded sidebands show the regions selected to estimate the background; (b) $\eta\pi^-$ effective mass distribution. The shaded region is an estimate of the background.

The $\eta\pi^-$ invariant mass spectrum in Fig. 1(b) is dominated by the $a_2(1320)$. The acceptance-corrected angular distribution in the Gottfried–Jackson reference frame shows a strong forward–backward asymmetry (not shown). This points towards interference between even and odd spins and indicates the existence of odd-L partial waves. A rank one partial wave analysis [1] up to spin 2 was done with 7 waves: S_0, P_0, P_-, D_0, D_- and P_+, D_+. The first set of 5 waves (not shown) has unnatural parity exchange [10] and is consistent with zero for $\eta\pi$-masses above 1.3 GeV/c^2. The unnatural parity exchange waves suffer from an eightfold mathematical ambiguity leading to the same angular distribution [11]. Since they are small, the natural parity exchange waves P_+, D_+ are only indirectly affected by this to the extent that the number of events in a given mass bin is constant. The

[1] The PWA formalism defines the amplitudes in the reflectivity basis, so they are characterized by the naturality (ε) of the exchanged particle, the orbital angular momentum of the $\eta\pi$ system (L), and the projection of the angular momentum L along the beam direction (M).

result of the partial wave analysis for the P_+ and D_+ waves and their phase difference are shown in Fig. 2.

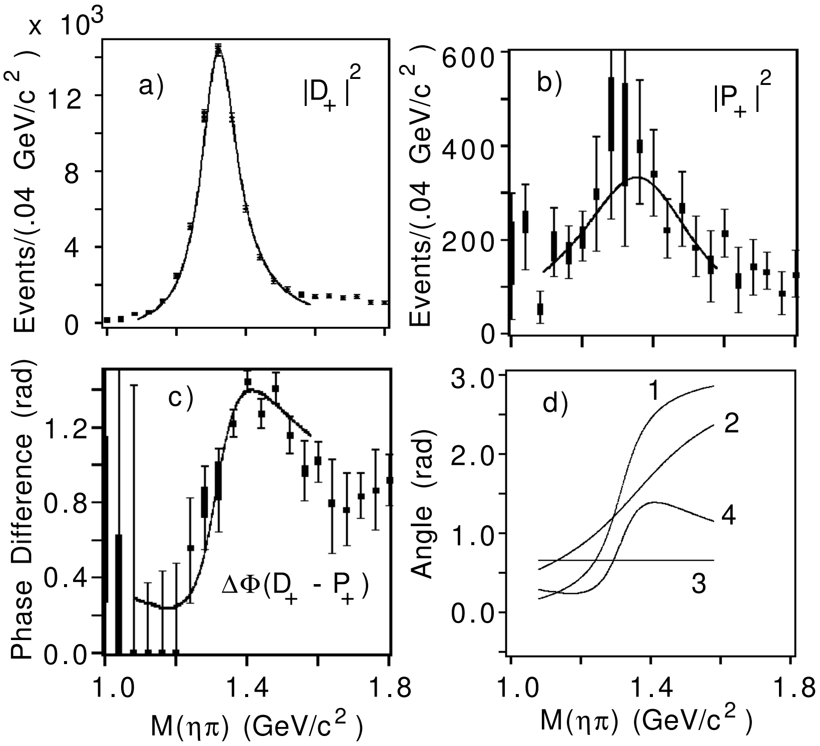

Fig. 2. Results of the partial wave amplitude analysis. Shown are (a) the fitted intensity distributions for the D_+ and (b) the P_+ partial waves, and (c) their phase difference $\Delta\Phi$. The range of values for the eight ambiguous solutions is shown by the central bar and the extent of the maximum error is shown by the error bars. Also shown as curves in (a), (b), and (c) are the results of the mass dependent analysis. The lines in (d) correspond to (1) the fitted D_+ Breit–Wigner phase, (2) the fitted P_+ Breit–Wigner phase, (3) the fitted relative production phase ϕ, and (4) the overall phase difference $\Delta\Phi$.

In order to understand the nature of the P_+ wave a mass-dependent fit to the results of the mass independent amplitude analysis was done. In this fit one assumes that the D_+ wave and the P_+ wave decay amplitudes are resonant and can be described by using relativistic Breit–Wigner forms[2]. The results of the fit are shown as smooth curves in Fig. 2. The mass and width of the $J^{PC} = 1^{-+}$ state are $(1370 \pm 16^{+50}_{-30})$ MeV/c^2 and (385 ±

[2] One further assumes that the production phase difference is constant.

40^{+65}_{-105}) MeV/c^2. This fit gives a χ^2/dof of 1.49. If one fits the data with a nonresonant P_+ wave one obtains a very poor fit with a χ^2/dof of 7.08. If one allows a mass-dependent production phase a χ^2/dof of 1.55 is obtained, but the production phase must have a very rapid variation with mass, requiring a slope of -4.3 radians/(GeV/c^2). This cannot be excluded but is not expected for any known model. The details of this analysis can be found in [12, 13]. In 1995 another data set was obtained with some 62 000 events. The data, although they have systematic differences, were analyzed in the same way as described above. The results for the J^{PC} determination, mass, width and phase difference are consistent with the results of the 1994 analysis. This is shown in Fig. 3.

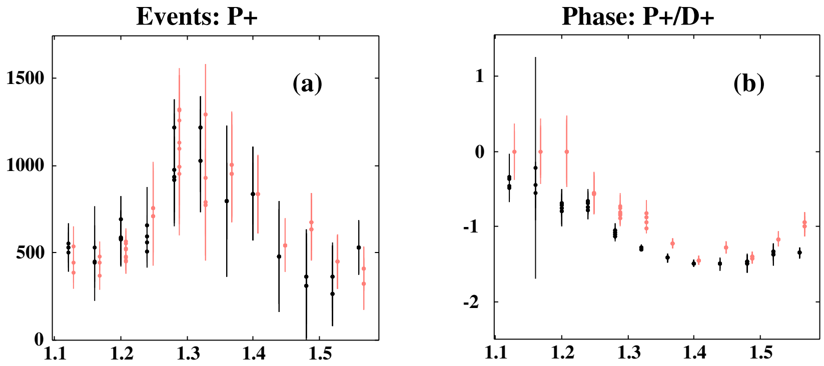

Fig. 3. Comparison of the $\eta\pi^-$ PWA results obtained on the 1994 data sample (dashed lines) and the 1995 data sample (solid lines). (a) The fitted intensity distributions for the P_+ wave; (b) its phase difference with the D_+ wave.

3. Study of the reaction $\pi^- p \to \pi^+\pi^-\pi^- p$

This data set (1994) contains 2.5×10^5 events after kinematic cuts were applied. The $\pi^+\pi^-\pi^-$ and $\pi^+\pi^-$ invariant mass spectra are shown in Fig. 4.

The three-pion spectrum is dominated by the well known $a_1(1260)$, $a_2(1320)$ and $\pi_2(1670)$ resonances. The two-pion spectrum shows strong signals from $\rho(770)$ and $f_2(1270)$. A partial-wave analysis of these data was performed. Each event is considered in the framework of the isobar model: an initial decay of a parent particle into a $\pi\pi$ isobar and an unpaired pion followed by the subsequent decay of the isobar. Each partial wave is characterized by the quantum numbers $J^{PC}[\text{isobar}]LM^{\varepsilon}$ — here J^{PC} are spin, parity and C-parity of the partial wave; M is the absolute value of the spin projection on the quantization axis; ε is the reflectivity (and corresponds to the naturality of the exchanged particle); L is the orbital angular mo-

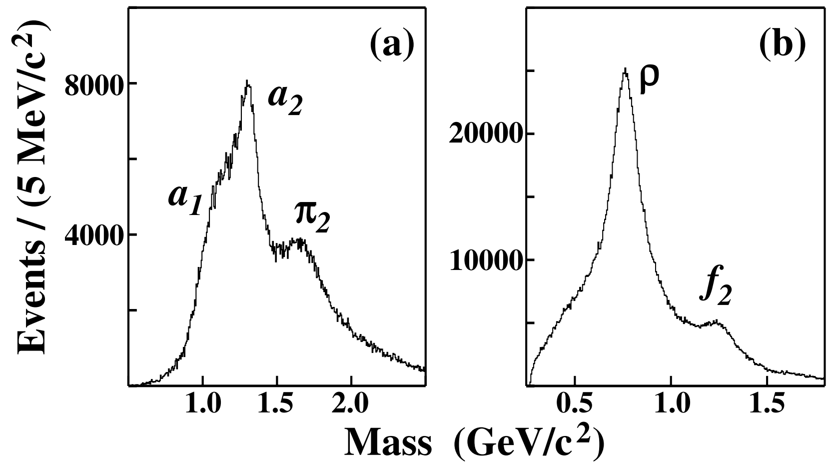

Fig. 4. Experimental effective mass distribution with acceptance correction: (a) $\pi^+\pi^-\pi^-$ mass spectrum, (b) $\pi^+\pi^-$ mass spectrum (two entries per event).

mentum between the isobar and the unpaired pion. It was determined that a minimal set of 21 partial waves is required in order to achieve a reasonable agreement between the experimental and predicted moments. This set takes into account all relevant decay modes of the known resonances. It includes three 0^{-+} waves, four 1^{++} waves, three 1^{-+} waves, two 2^{++} waves, seven 2^{-+} waves, one 3^{++} wave, and a non-interfering isotropic wave (which turned out to be rather small). The 1^{-+} waves were found to be essential for the description of the moments.

The acceptance-corrected numbers of events for the major non-exotic spin-parity states predicted by the PWA fit are shown in Fig. 5.

The $J^{PC} = 1^{++}$ wave corresponding to the $a_1(1260)$ meson is dominant and accounts for almost half of the total number of events in the sample. The $a_2(1320)$ is prominent in the $J^{PC} = 2^{++}$ waves, and the $\pi_2(1670)$ dominates the $J^{PC} = 2^{-+}$ waves. The $J^{PC} = 0^{-+}$ spectrum is quite complex. Its shape below 1.6 GeV/c^2 is very sensitive to the choice of the $\pi^+\pi^-$ S-wave parameterization. Despite this complexity, the $\pi(1800)$ state is clearly seen in the spectrum.

The intensities of the exotic waves are shown in Fig. 6.

All three $1^{-+}[\rho(770)]P$ waves with $M^\varepsilon = 0^-, 1^-, 1^+$ (denoted as P_0, P_-, and P_+) show broad enhancements in the 1.1–1.4 GeV/c^2 and 1.6–1.7 GeV/c^2 regions. At the same time, the $1^{-+}[f_2(1270)]D1^+$ wave (not shown) is consistent with zero. Monte Carlo studies showed that there is considerable leakage from the $a_1(1260)$ into these waves at low masses. However, the 1.6 GeV/c^2 region does not suffer from this.

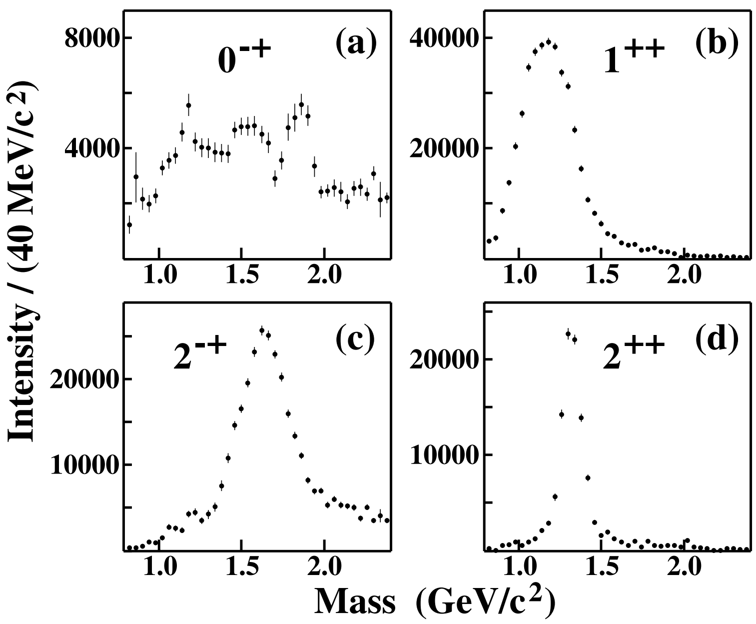

Fig. 5. Combined intensities of all (a) 0^{-+} waves, (b) 1^{++} waves, (c) 2^{-+} waves, (d) 2^{++} waves.

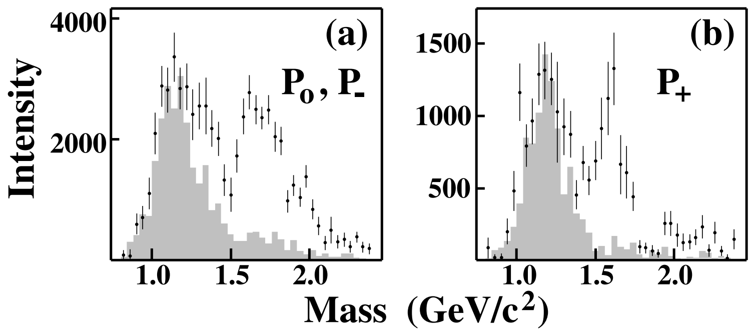

Fig. 6. Wave intensities of the $1^{-+}[\rho(770)]P$ exotic waves: (a) the $M^{\varepsilon} = 0^-$ and 1^- waves combined, (b) the $M^{\varepsilon} = 1^+$ wave. The PWA fit to the data is shown as the points with error bars and the shaded histograms show estimated contributions from all non-exotic waves due to leakage.

The phase difference between the $1^{-+}[\rho(770)]P1^+$ wave and all other significant natural parity exchange waves indicates a rapid increase in the phase of the 1^{-+} wave across the 1.5–1.7 GeV/c^2 region; this is consistent with resonant behaviour.

To determine the resonance parameters, a series of two-state χ^2 fits of the $1^{-+}[\rho(770)]P1^+$ and $2^{-+}[f_2(1270)]S0^+$ waves as a function of mass was made. Both waves are parameterized with relativistic Breit–Wigner forms including Blatt–Weisskopf barrier factors. In addition to Breit–Wigner phases, a production phase difference which varies linearly with mass is assumed. The fit yields $\chi^2 = 25.8$ for 22 degrees of freedom, with the production phase difference between the two waves being almost constant throughout the region of the fit. If instead the 1^{-+} wave is assumed to be non-resonant (with no phase motion), then the fit has $\chi^2 = 50.8$ for 22 degrees of freedom, and requires a production phase with a slope of 7.6 radians/(GeV/c^2). Such rapid variation of the production phase makes a non-resonant interpretation of the 1^{-+} wave unlikely.

The fitted mass and width of the 1^{-+} state are $M = (1593 \pm 8^{+29}_{-47})$ MeV/c^2 and $\Gamma = (168 \pm 20^{+150}_{-12})$ MeV/c^2. The error values correspond to statistical and systematic uncertainties, respectively. The systematic errors were estimated by fitting the PWA results obtained for different sets of partial waves and different rank of the PWA fit. A more detailed description of this analysis can be found in [14].

In 1995 a second data set was obtained with much larger statistics, 5×10^6 events. The three-pion and two-pion mass spectra are shown in Fig. 7. They are remarkably similar to the data shown in Fig. 4 and will allow a much more detailed partial wave analysis which is in progress now.

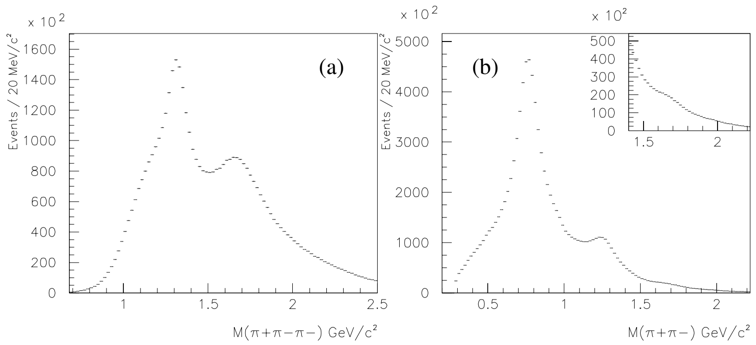

Fig. 7. Experimental effective mass distribution for 1995 data sample: (a) $\pi^+\pi^-\pi^-$ mass spectrum, (b) $\pi^+\pi^-$ mass spectrum (the $\rho_3(1690)$ region is shown in inset).

4. Study of the reaction $\pi^- p \to \eta'(959)\pi^- p$

This data set contains, after kinematic cuts, 6 040 events (1995 data) of the type $\pi^- p \to \eta'(959)\pi^- p$ where $\eta'(959) \to \eta\pi^+\pi^-$ and $\eta \to \gamma\gamma$. Shown in Fig. 8 are the 2γ, $\eta\pi^+\pi^-$ and $\eta'\pi^-$ effective mass distributions for the data.

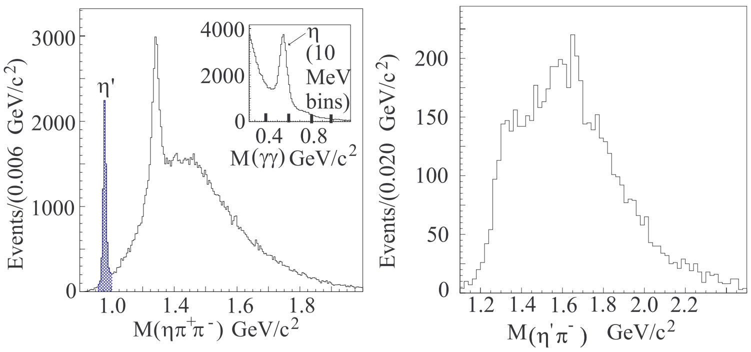

Fig. 8. Distribution of the 2γ effective mass (inset), the $\eta\pi^+\pi_-$ effective mass (left) and the $\eta'\pi^-$ effective mass (right).

Clear evidence for the η is seen in the 2γ mass distribution. These photon pairs were kinematically constrained to be consistent with an η. The resulting $\eta\pi^+\pi^-$ mass distribution shows a clear η' signal. After constraining the $\eta\pi^+\pi^-$ system to be consistent with the η', the resulting $\eta'\pi^-$ mass distribution shown in the figure 8 contains structure in the 1.6 GeV$/c^2$ region.

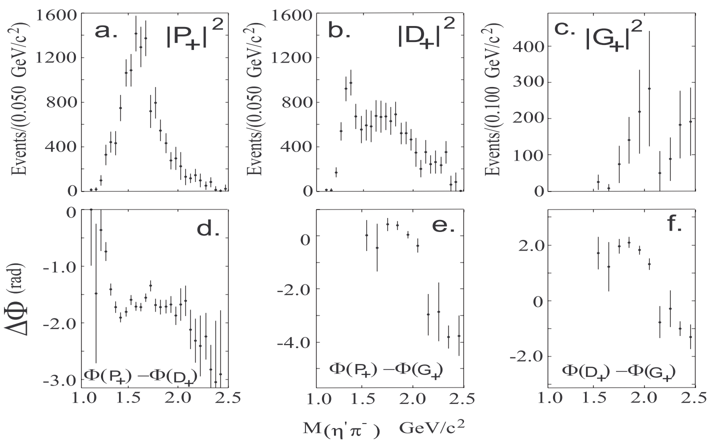

Fig. 9. Natural parity exchange waves from the mass-independent $\eta'\pi^-$ PWA.

Amplitude analyses were carried out using the standard E852 PWA package. The waves used in the fit included, for natural parity exchange ($\varepsilon = +1$), P, D, and (in some cases) G waves; and for unnatural parity exchange, ($\varepsilon = -1$), S, P, and D waves. We also assume $|M| \leq 1$. (Note that for $\varepsilon = +1$, $M = 0$ is forbidden.) In this paper, we denote the natural parity waves as P_+, D_+, and G_+; and the unnatural parity waves as S_0, P_0, and D_0 for the $M = 0$ waves and P_- and D_- for the $|M| = 1$ waves.

The main features of the amplitudes are: the strong production of the P_+ wave in Fig. 9a; structure in Fig. 9b in the $a_2(1320)$ region and at higher mass; and significant structure in the phase difference plots of Figs. 9d, e, and f.

The unnatural parity exchange waves (not shown) are all quite small although they are required to obtain good fits to the data. We find a satisfactory description of the data if we assume the presence of a single exotic P-wave resonance, a pair of D-wave resonances, and a G-wave resonance. A preliminary fit leads to the values for the mass and width of the 1^{-+} exotic state of 1598 ± 9 MeV/c^2 and 380 ± 22 MeV/c^2 respectively. This is most likely the same state (the $\pi_1(1600)$) observed previously [14] decaying to $\rho\pi$. The fitted parameters of the lower-mass D-wave resonance are consistent with those of the $a_2(1320)$; and the parameters of the G-wave state ($M = 2030 \pm 40$ MeV/c^2 and $\Gamma = 320 \pm 140$ MeV/c^2) are consistent with production of the $a_4(2040)$.

Fits were carried out with two P-wave resonances. The fits did improve somewhat when the $\pi_1(1400)$ was included but since a satisfactory fit was attained without this second state, we can only say that our data is consistent with its production but the fit does not require it. The second D-wave resonance in the fits is very broad ($\approx$500–600 MeV/c^2 wide) and peaks around 1.8 GeV/c^2. Although this may be a resonant state, the very broad width suggests that it represents the production of a slowly varying non-resonant D-wave system.

REFERENCES

[1] N. Isgur *et al.*, *Phys. Rev. Lett.* **54**, 869 (1985).

[2] N. Isgur, J. Paton, *Phys. Rev.* **D31**, 2910 (1985).

[3] T. Barnes *et al.*, *Nucl. Phys.* **B224**, 241 (1983).

[4] F. E. Close, P. R. Page, *Nucl. Phys.* **B443**, 233 (1995).

[5] T. Barnes *et al.*, *Phys. Rev.* D**D52**, 5242 (1995).

[6] M. Chanowitz, S. Sharpe, *Nucl. Phys.* **B222**, 211 (1983).

[7] R. L. Jaffe, *Phys. Rev.* **D15**, 267 (1977).

[8] P. Lacock *et al.*, *Phys. Rev.* **D54**, 6997 (1996); C. Berbard *et al.*, *Nucl. Phys.* (Proc. Suppl.) **B53**, 228 (1997).

[9] S. Teige *et al.*, *Phys. Rev.* **D59**, 012001 (1999).

[10] S. U. Chung, T. L. Trueman, *Phys. Rev.* **D11**, 633 (1975).

[11] E. Barrelet, *Nuovo Cimento* **A8**, 331 (1972).

[12] D. R. Thompson *et al.*, *Phys. Rev. Lett.* **79**, 1630 (1997).

[13] S. U. Chung *et al.*, *Phys. Rev.* **D60**, 092001-1 (1999).

[14] G. S. Adams *et al.*, *Phys. Rev. Lett.* **81**, 5760 (1998).